Review on one-dimensional nanostructures prepared by electrospinning and atomic layer deposition

Imre Miklós Szilágyi[1,2*] and Dávidné Nagy[3]

[1]Budapest University of Technology and Economics, Department of Inorganic and Analytical Chemistry, Szent Gellérttér 4., Budapest, H-1111, Hungary;
[2]MTA-BME Technical Analytical Research Group of the Hungarian Academy of Sciences, Szent Gellérttér4., Budapest, H-1111, Hungary;
[3]University of Edinburgh, The King's Buildings, Mayfield Road, Edinburgh, EH9 3JL, UK

E-mail: imre.szilagyi@mail.bme.hu

Abstract. This paper reviews the various 1D nanostructures, which were prepared by electrospinning and atomic layer deposition (ALD). On the one hand, electrospinning served to make sacrificial polymer templates for the ALD growth; and thus various single or multilayer inorganic nanotubes were obtained. On the other hand, polymer, polymer/inorganic or inorganic nanowire templates were produced by electrospinning. By a consecutive ALD reaction various core/shell nanowires were synthesized.

1. Introduction

One dimensional (1D) nanostructures have attracted considerable attention in the recent decades. They have very interesting size-dependent chemical, mechanical, electrical, optical, magnetic, etc. properties, which are due to their one dimensionality. Owing to their unique features, they have been used in a large number of fields, including optoelectronics, nanoelectronics, plasmonics, medical diagnostics, catalysis, drug delivery, therapeutics, separations, and sensing [1-4].

Historically, some decades ago materials synthesis studies focused a great deal to prepare good-quality single crystals. Nevertheless, some materials grow easier in one dimension, rather than in 3D; however, this was considered a problem and the growth of nanowires was tried to be eliminated. The research on nanowires and nanotubes, accelerated in the 1990s, as the nanosized features moved into the center of interest [5-8].

By now, numerous ways have been developed to prepare 1D nanostructures, i.e. spontaneous growth, vapor-liquid-solid (VLS) route, templating on patterned surfaces, growth in porous channels, using self-assembly templates, templating against existing 1D nanostructures, preparation from the vapor phase, solvothermal methods, growth oriented by capping agents, self-assembly of nanoparticles and electrospinning. These are bottom-up approaches, but also top-down methods are available, e.g. isotropic deformation of amorphous or crystalline material, anisotropic etching of single crystals to prepare e.g. grooves, and lithography. These synthesis methods can result in nanorods (with aspect ratios, AR,usually below 20), nanowires (AR>20), nanobelts, nanotubes, nanoneedles, whiskers [5, 9, 10].

Among the various synthesis methods, electrospinning is a convenient and widely used method to obtain 1D nanostructures in a short time and large scale. By this way, polymer, polymer/inorganic and inorganic nanofibers can be prepared. Atomic layer deposition (ALD) is becoming a key tool in nanotechnology, and it can be both a preparation method for 1D nanomaterials and also as a unique technique to program the surface properties of 1D nanosystems.

This paper reviews the various 1D nanostructures, where the synthesis relied both on electrospinning and ALD. Electrospinning served either to make a sacrificial template for the ALD layer to obtain nanotubes, or provided a nanowire template for ALD to prepare core/shell materials.

2. Electrospinning

Electrospinning is a convenient and cost-effective method for the fabrication of nanofibers. The earliest studies date back to the 1930s, but for long the technique remained unexploited. It was newly discovered in the 1990s and has gained a lot of attention since then.

The origin of the method stems from the early "electrostatic spinning" terminology; implying, on the one hand, the application of electrostatic force and, on the other hand, the spinning movement of the ejected polymer solution [11]. The experimental setup basically consists of four main parts: the power supply for achieving high voltage, the needle electrode connected to the polymer solution, the capillary for delivering the precursor solution and the earthed collector (figure 1a) [12].High voltage is applied between the ejection site and the earthed collector. The polymer solution is conducted through a syringe and charged by the applied potential by means of which it starts to form a Taylor cone. The spinning movement is the result of the counteraction of the electrostatic force and the surface tension. By the time the polymer reaches the collector the liquid jet has lost its solvent content and has been elongated due to electrostatic repulsion. The properties of the final product depend upon influencing factors including the characteristics of the polymeric solution, the operation conditions and the surrounding temperature and humidity [13, 14].

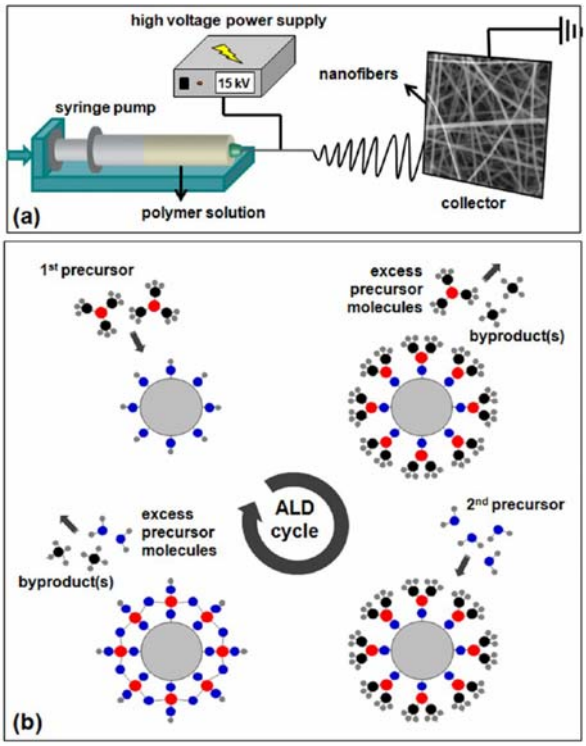

Figure 1. Schematic representation of (a) an electrospinning setup; (b) an atomic layer deposition (ALD) reaction cycle. (Reprinted with permission from [75]. Copyright 2014 American Chemical Society.)

Electrospinning received much attention recently owing to its low cost, high efficiency and good reproducibility [11]. Numerous research areas try to exploit the benefits of what this technique could offer. The nanofibers in general could play key role in environmental protection [15]. In the oil spill

cleaning, nanofibrous highly porous membranes are used as sorbents taking advantages of the various functionality, and high uptake capacity could be achieved by electrospun nanofibers [11]. The so-called colloidal nanofibers are considered as good candidates in the field of filtration, adsorption or even as sensors due to the special surface roughness and enhanced properties introduced by the colloidal particles [16]. Besides the high specific surface area, the nanofibers exhibit outstanding charge transport properties owing to their high aspect ratio character, which enables less interfacial interaction of the travelling electrons at grain boundaries. This feature could highly promote the efficiency of light-harvesting devices, such as dye sensitized solar cells (DSSC) or photocatalytic systems [17, 18]. In the opto-electronic industry a specific class of electrospun nanofibers, the conjugated polymer filaments, could potentially revolutionize future devices by providing the attractive possibility to fabricate flexible and light-weight products [13, 19]. Electrospinning attracted substantial interest in the medical research as well, especially in the development of effective drug delivery systems where the high encapsulation and loading efficiency of a wide range of drugs are desired [15].

3. Atomic layer deposition

The basic theory of ALD has been developed already in the 1950s by Aleskovskii in the USSR. He and Koltsov made the first experiments in the 1960s with the method they called molecular layering (ML). Independent of them, Suntola and coworkers developed also the basic principles of ALD in Finland in the 1970s, and it was them who enabled ALD to be used widely in the industry.At first they used only elemental precursors and the method was named atomic layer epitaxy (ALE) [20-23].

The first industrial application of ALD was thin film electroluminescent (TFEL) flat-panel displays. Almost from the beginning, ALD has been researched to be utilized in various other fields as well (e.g. catalysis), but the real international interest has arrived only in the 1990s, when ALD was considered to be a key future method in the semiconductor industry. As the dimensions decreased in silicon-based microelectronics devices, serious conformality problems with the thin films deposited by the existing methods were foreseen to arise in the coming years. Therefore, ALD was selected to be a major method in depositing thin films for several fields, including high dielectric constant gate oxides in metal oxide semiconductor field effect transistors (MOSFETs), copper diffusion barriers in backend interconnects, high aspect ratio trench structures of memory capacitors, etc. Already in the 2000s, major semiconductor companies used ALD partly in their manufacturing technologies. Also in the 2000s, ALD has started to gain interest in nanotechnology, e.g. in sensors, fuel cells, solar cells, catalysis, nanocoatings, displays, LEDs, nanocomposites, nanodevices, etc. [24-28].

A general ALD reaction has four consecutive steps (figure 1b): (i) the first precursor is pulsed into the reactor, which chemisorbs on the surface of the substrate; (ii) the unreacted precursor or reaction byproducts are removed by an inert gas purge and/or by evacuation; (iii) the second precursor is purged, which reacts with the first precursor solely on the surface; (iv) the unused second precursor and the reaction byproducts are removed [29-32].

ALD and chemical vapor deposition (CVD) have many similarities, yet there are several distinctive features, which make ALD unique. In ALD the adsorption of reactants is self-limited and the various precursors meet only on the surface of the substrate [33, 34].

The self-limiting growth leads to the many advantages of ALD. ALD can provide thickness control at an atomic level, as the film thickness can be programmed easily by the number of the ALD cycles. Not only the thickness, but also the composition of the film can be controlled precisely. With ALD, finely tuned doping of thin films or preparation of nanolaminates is easily achievable. ALD can prepare extremely conformal layers, and due to the volatile precursors and self-limiting growth even high aspect ratio structures can be uniformly coated. In ALD there is no shadow effect, which is a hindrance of various other physical and chemical gas phase thin films deposition methods; where, if there is an object between the source and the target, it can reduce the growth rate behind it [35-39].

During the recent decades, ALD precursor chemistry has developed rapidly. ALD can use solid, liquid or gaseous precursors. If the partial pressure of the solid or liquid precursors is low at room

temperature, they can be heated to have better sublimation or evaporation conditions. The precursors can be elements, molecules, radicals. By now the variety of materials that can be grown by ALD is very rich. ALD can be used to deposit elements (Au, Ag, Pt, Ru, Fe, etc.), binary compounds (e.g. oxides, nitrides, carbides, sulfides, fluorides, like Al_2O_3, TiO_2, ZnO, HfO_2, GaN, TaC, CaS, SrF_2, etc.), ternary compounds (e.g. $MgAl_2O_4$, TiAlN). Even polymers and organic materials can be grown by ALD. Molecular layer deposition (MLD), a recent version of ALD, where a molecular fragment is deposited during each ALD cycle, can increase the number of ALD prepared materials even further with organic or organic/inorganic (e.g. zincones, alucones) polymers [40-47].

The usual reaction temperature is between 100-400°C, and the ideal reaction temperature zone is often described by the so-called ALD window. The elevated temperature is useful for increasing the precursor and the substrate reactivity, and also to accelerate the sorption processes. However, ALD reactions can be performed at both higher and lower temperatures as well. Low temperature ALD makes it possible to coat heat sensitive substrates, e.g. polymers, biomaterials [48-50].

Considerable efforts have been made to extend the possibilities of traditional ALD to meet the industrial requirements. Plasma or radical enhanced ALD made it possible to deposit Ag or Au, which were not possible by thermal ALD. Usually ALD reactions take place in vacuum, but it is also possible to grow thin films by atmospheric pressure ALD, which makes it much easier to adapt the ALD reaction to other industrial processes. Especially in the semiconductor industry, it might be vital not to grow thin films on the complete substrate but only on parts of it, and this can be achieved by area selective ALD. The slow growth rate of ALD can be overcome by coating a large numbers of substrates at the same time, or by using roll-to-roll or spatial ALD technology [51-54].

As ALD allows deposition of uniform thin films on three dimensional (3D) objects with thickness control of sub-nanometer precision, ALD provides new strategies in modifying the properties of nanoscaled materials and new synthetic routes to novel nanostructures. By now, outstanding results have been achieved by ALD in nanotechnology: preparing or coating nanodots, nanotubes, nanowires, nanolaminates, nanoporous materials, inverse opal structures, various nanocomposites, bionano materials, etc. [55-60].

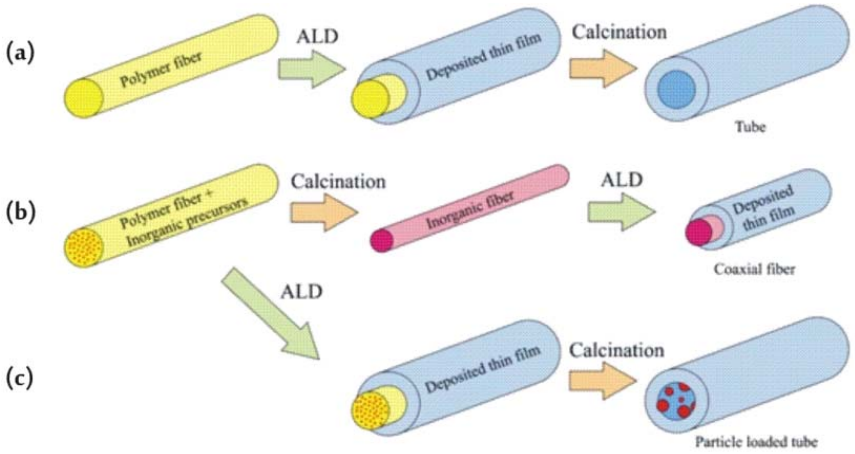

Figure 2. The preparation of (a) nanotubes;(b) core/shell nanowires and (c) particle loaded nanotubes by electrospinning and ALD [61]. (doi: 10.1088/0957-4484/20/3/035602. © IOP Publishing.Reproduced with permission. All rights reserved.)

4. 1D nanostructures obtained by electrospinnning and ALD

The combination of electrospinning and ALD is a powerful tool to prepare nanotubes and core/shell 1D nanostructures, which is clearly reflected by the dozens of already published studies. The various steps for preparing nanotubes and core/shell nanofibers by electrospinning and ALD are summarized

in figure 2 [61]. When a core polymer nanofiber is produced by electrospinning, and a shell layer is deposited by ALD, an organic/inorganic core/shell fiber is obtained. If the polymer core is removed by e.g. annealing, a nanotube is prepared (figure 2a). If the electrospinning solution contains inorganic salts as well, then a polymer/inorganic fiber can be electrospun. After annealing the polymer part, the as-obtained inorganic nanofibers can also serve as substrate for the ALD reaction and hence inorganic core/shell nanofibers is produced. It is also possible to load nanoparticles into nanotubes by combining electrospinning and ALD (figure 2b). For this, the as-spun polymer/inorganic nanofiberis covered with an ALD layer before removing the polymer part. If the inorganic salt has appropriate (i.e. low enough) concentration in the electrospinning solution, then instead of a core/shell nanofiber a particle-loaded nanotube will be the product (figure 2c).

In the next sections, at first nanotubes, then core/shell nanofibers are reviewed, which have been obtained by the synergy of electrospinning and ALD.

4.1. Inorganic nanotubes prepared by electrospinning and ALD

Al_2O_3 nanotubes with tuned wall thickness represent one of the first examples of 1D nanostructures, which were produced by combining electrospinning and ALD. 200-400 nm thick polyvinyl alcohol (PVA) nanofibers were electrospun, and Al_2O_3 nanofilms were deposited on the fibers by ALD (60°C, trimethyl aluminium (TMA) and H_2O as precursors). After removing the polymer core by annealing at 400 °C for 24 h, Al_2O_3 nanotubes were obtained with tuned wall thickness (14-28 nm) [62].

Al_2O_3 nanotubes with porous, coral-like structure and extremely high specific surface were produced using the same precursors, but with a different polymer core removal process (figure 3). PVA nanofibers (340 nm thick) were obtained by electrospinning. They were covered uniformly by 25, 50 and 100 nm Al_2O_3 films by ALD. The PVA core was not removed by annealing, but by dissolution in water at varying temperatures and times (20-100°C and 30-180 min, respectively). From 40°C, the polymer swelled in water causing cracks on the shell Al_2O_3 layer. As the dissolved polymer migrated out, a complex channel structure was formed on the tube walls, resembling a nanocoral structure. The as-formed porous nanotubes grew in diameter (1300 nm), and the material had very high specific surface, i.e. 323 m^2/g. This structure was suggested to be beneficial to prepare porous materials for filtration or catalysis [63].

PVA electrospun nanofibers (300 nm thick) served as a template also for a multilayer Al_2O_3 (18 nm)/ZnO (8.5-39 nm)/Al_2O_3 (22 nm) nanotubular structure. Al_2O_3 (TMA and H_2O) and ZnO (diethyl zinc (DEZ) and H_2O, 45 and 65°C, respectively) were deposited by ALD. The PVA core was removed by annealing at 450°C for 12 h, or by dissolution in H_2O for 12 h. After this the Al_2O_3/ZnO/Al_2O_3multilayer nanotubes were annealed at 700°C for 12 h, and during that ZnO diffused into both the inner and the outer Al_2O_3 layers. The vacancy supersaturation and Kirkendall void production resulted in two isolated $ZnAl_2O_4$ spinel nanotubes. The Kirkendall gap between the tube-in-tube structure was influenced by the intermediate ZnO layer [64].

ZnO nanotubes were prepared using polyvinyl pirrolidone (PVP) nanofibers as sacrificial templates as well, but in this case the obtained nanotubes were not multilayer, but single. 180 nm ZnO layers were grown by ALD (70°C, DEZ and H_2O) onto the 630 nm thick PVP nanofibers, then the PVP core was eliminated by annealing at 500°C for 4 h. The ZnO layer consisted of 30 nm ZnO nanoparticles, and the calcinations lead to their oriented grain growth. As a result the wall of the free standing ZnO nanotubes were composed of 200 nm ZnO nanoplatelets [65].

Besides PVP, also polyacrylnitrile (PAN) as-spun nanofibers were templates for ZnO nanotubes. On the 100-150 nm electrosun PAN nanofibers 10, 30 and 50 nm ZnO films were deposited by ALD (150°C, DEZ and H_2O). If the PAN/ZnO composite was only annealed at 500°C for 2h to remove PAN, the thin ZnO walls collapsed. Thus, an O_2 plasma treatment was applied before the annealing, and the nano tubular structure was well preserved. The ZnO nanotubes were tested as gas sensors to ethanol (EtOH). The ZnO nanotube with 10 nm wall thickness was wholly depleted, and due to this it was the most sensitive to 100 ppm EtOH with an extreme response of 1184, and subsecond response time between 350-500°C. The sensor was selective to EtOH, relative to H_2 [66].

Using PAN nanofibers as core materials, gas sensitive SnO_2 nanotubes were obtained as well. 100-200 nm thick PAN nanofibers were electrospun, onto which 8, 22 and 37 nm SnO_2 layers were grown by plasma enhanced (PE) ALD (100°C, dibutyltindi acetate (DBTDA) and O_2 plasma). The amorphous as-deposited SnO_2 became crystalline during annealing (700°C, 1h), and the polymer core was eliminated as well. Similar to ZnO nanotubes, the SnO_2 nanotubes with the smallest wall thickness had the highest response (188) to 100 ppm EtOH and shortest response time (few seconds). This was due to the complete electron depletion and effective gas diffusion through the permeable wall, composed of interconnected SnO_2 nanoparticles. The sensors were selective to EtOH in the presence of reducing gases (H_2, CO, NH_3), but not in the case when oxidizing gases (NO_2) were present [67].

The same group prepared a continuously aligned and assembled structure, i.e. a ca. 50 μm thick yarn, by electrospinning, aligning and twisting PAN nanofibers. They deposited SnO_2 films by the above mentioned PE-ALD process on the PAN yarn then annealed the composites at 700°C. Hence, the obtained SnO_2 yarn consisted of nanotubes with a diameter and wall thickness of 500 and 70 nm, respectively (figure 4). The main advantage of the yarn was its easy handling, which was demonstrated in preparing a H_2 sensitive gas sensor [68].

TiO_2 nanotubes were prepared as well by electrospinning and ALD. 500 nm PVP fibers were electrospun, onto which 60 nm TiO_2 was deposited by ALD (70°C, $Ti(O_iPr)_4$ and H_2O). To remove the polymer, the PVP/TiO_2 fiber was annealed at 500°C for 4h. During this the as-grown amorphous TiO_2 crystallized into 16 nm anatase platelet grains, parallel to the direction of the tube axis [69].

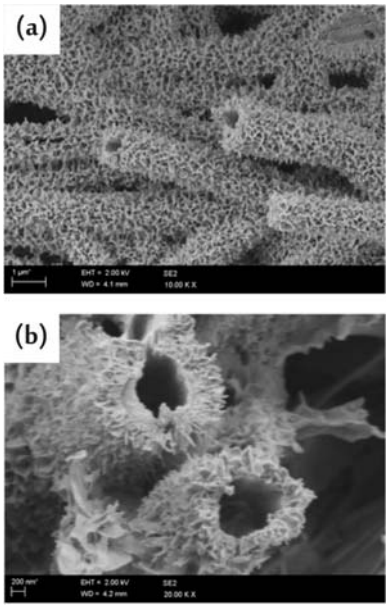

Figure 3.SEM images of Al_2O_3nanocoral formed after dissolving the PVA core from PVA/ Al_2O_3 core/shell nanofibersat (a) lower and (b) higher magnifications. (Reprinted from [63] with kind permission of Springer Science and Business Media.)

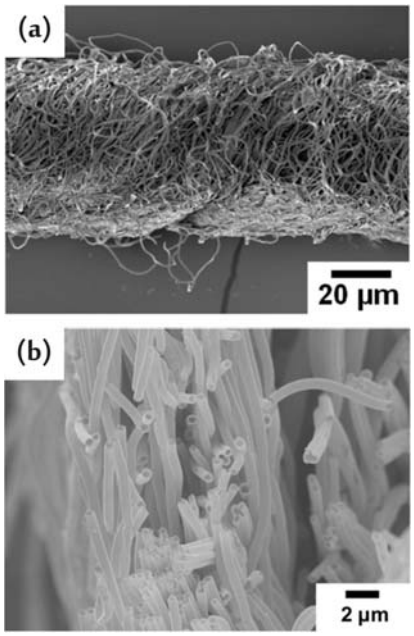

Figure 4. SEM images of (a) SnO_2 nanotube yarn; (b) individual SnO_2 nanotubes [68]. (doi: 10.1088/0964-1726/20/10/105019. © IOP Publishing. Reproduced with permission. All rights reserved.)

TiO_2 nanotubes served a basis of an Ag/Al_2O_3/TiO_2 nanotube composite too. 15-80 nm Ag nanoparticles (NPs) were obtained by sol-gel method and mixed in a polyethylene oxide (PEO) solution. From this Ag NP embedded PEO nanofibers (650 nm thick) were electrospun. Ca. 0.15-1.5 nm Al_2O_3 layer was deposited on the fibers by PE-ALD (65°C, TMA and O_2 plasma), then 4-14 nm

TiO_2 was grown by PE-ALD ($Ti(O_iPr)_4$ and O_2 plasma). The PEO polymer was dissolved in water and the $Ag/Al_2O_3/TiO_2$ nanotube was annealed at 500°C for 1 h. This hybrid system was tested in a DSSC applications), and showed an enhanced light absorption and an increased photocurrent generation, compared to Ag/TiO_2 nanotubes. The plasmonic effect of Ag NPs could be controlled with the thickness of the dielectric Al_2O_3 spacer between the Ag NPs and the dye molecules [70].

SnO_2/TiO_2 multilayer nanotubes were prepared as lithium ion battery anodes. PAN nanofibers (200-300 nm thick) were electrospun, onto which 12 nm SnO_2 and 22 nm TiO_2 layers were deposited consecutively by PE-ALD (100°C, dibutyltindi acetate and O_2 plasma, $Ti(O_iPr)_4$ and O_2 plasma, respectively). The PAN core was removed by annealing at 700°C for 1 h. While pure SnO_2 nanotubes disintegrated into nanoparticles during electrochemical charging/discharging, the TiO_2 encapsulation of SnO_2 prevented this. The high capacity of SnO_2 and the superior cycling performance of TiO_2 were synergistically combined in the SnO_2/TO_2 double shell nanotube electrode [71].

HfO_2 is another material from which nanotubes were produced by electrospinning and ALD. The core polymer nanofibers (70 or 330 nm) were made of nylon 6,6. The fibers were covered by 15 or 70 nm HfO_2 layers by ALD (200°C, $Hf(NMe_2)_4$ and H_2O). The polymer core was removed by heating at 500°C for 2 h to obtain HfO_2 nanotubes [72].

4.2. Organic core/inorganic shell nanofibers produced by electrospinning and ALD

In a pioneer study, the etching of electrospun nylon nanofibers by the most common ALD precursor, i.e. TMA, was investigated, and also it was studied how it could be prevented. Nylon nanofibers were obtained from polyamide-6 (PA-6) solution. Al_2O_3 (60 and 90°C, TMA and H_2O), and ZnO (60°C, DEZ and H_2O) were grown on the fibers by ALD, while an organic/inorganic hybrid layer (120°C, TMA and gylcidol) by MLD. The TMA precursor is highly reactive and it caused significant fiber degradation. When ZnO was deposited prior to Al_2O_3, it decreased the corroding effect of TMA, yet a certain part of TMA could still reach the core polymer by diffusing through the polycrystalline ZnO. In contrast, protecting the fibers by both the ZnO and the MLD layer was effective and the shape of the original polymer fibers was maintained [73, 74].

Electrospun nylon 6,6nanofibers (80, 240 or 650 nm thick) were used also as templates for 90 nm ZnO nanolayers grown by ALD (200°C, DEZ and H_2O). The electrospun nylon/ZnO fibers formed a flexible and mechanically stable mat. Their photocatalytic activity increased with a decrease in the core polymer diameter [75].

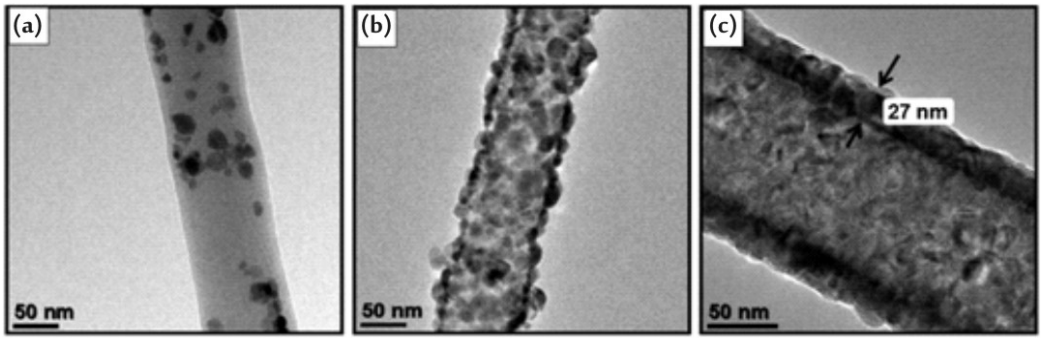

Figure 5. TEM images of electrospun nylon nanofibers coated (a) with remote ZnO nanoparticles (NPs); (b) densely with ZnO NPs; (c) with 27 nm thick layer of ZnO NPs. (Reproduced from [76] with permission of The Royal Society of Chemistry.)

The photocatalytic activity of ALD deposited ZnO (200°C, DEZ and H_2O) nanoparticles or nanofilms on similar, electrospun 80 nm thick nylon 6,6 nanofibers was investigated further. Varying the ALD parameters, i.e. normal dose and dynamic vacuum, increased dose and dynamic vacuum, normal dose and static vacuum, the polymer nanofibers were decorated with remote 20 nm ZnO NPs,

with densely packed ZnO NPs, or with a continuous 27 nm thick ZnO layer consisting of ZnO NPs (figure 5). All composites were good photocatalysts, and the nylon nanofibers packed densely with ZnO NPs had the largest activity, due to their highest specific surface [76].

The application of ALD ZnO coated electrospun fibers was studied further in photocatalysis. 1000 nm thick polysulfone (PSU) as-spun fibers were coated by ALD with distinct 10 nm ZnO nanoparticles (quantum dots), and also with 43, 56 and 75 nm ZnO nanocoatings built up by this particles. The PSU/ZnO composite with the thickest ZnO layer had the highest photocatalytic activity. The role of oxygen vacancies (V_Os) and Zn interstitials (Zn_i) were investigated. As the ALD cycle number and the ZnO thickness increased, the number of V_Os grew, while the density of Zn_i remained basically the same. It was concluded that V_Os are more effective in the context of photocatalysis than Zn_is and related defects [77].

In a recent study,a flexible mat of 655 nm thick electrospun PAN nanofibers was covered with 60 nm ZnO thin films by atomic layer deposition. This ZnO layer served as seed in a consecutive hydrothermal process, where 25 nm thick and 600 nm long single crystalline ZnO nanowires were grown on the PAN/ZnO composite fibers. The as-obtained hybrid had excellent photocatalytic activity, which was due to the synergy of the catalytic activity at surface defects (of ALD ZnO seed coating), of the valence band and the conduction band (of ZnO nanoneedles) [78].

Besides ZnO and Al_2O_3, TiO_2 nanofilms were also deposited on electrospun polymer fibers. It was studied how the precursors-substrate interactions during ALD coating influenced the mechanical properties of the fibers. Al_2O_3, ZnO and TiO_2 thin films were deposited by ALD (50 and 150°C) on nylon nanofibers (200 nm in diameter) prepared by electrospinning. Smaller ALD precursors (TMA for Al_2O_3, $TiCl_4$ for TiO_2) diffused into polymer and formed particles there, while larger precursors (DEZ for ZnO and $Ti(O_iPr)_4$ for TiO_2) rather formed a film on the surface of the polymer. The diffusion of oxide precursors into the polymer increased Young's modulus and decreased the ultimate strain [79].

Such nanofibers were prepared by electrospinning as well, which contained both PAN and an iron salt (Fe phtalocyanine). Onto these, TiO_2 was deposited by low temperature ALD (50°C, $TiCl_4$ and H_2O), and the hybrid was pyrolyzed in N_2 at 900 °C for 2 h. As a result core/shell Fe-containing carbon/TiO_2 composite fibers were obtained. These were used as electrocatalysts for the oxygen reduction reaction (ORR) of fuel cells. Adding Ti species to the Fe-C fibers increased the mass activity of the ORR and decreased the production of the side product H_2O_2, i.e. increased the selectivity of the reaction [80].

Al_2O_3 coated Si/C nanofibers are another examples, where not polymer but carbon fibers were in the core. 30-50 nm Si nanoparticles were mixed with PAN, and 150-300 nm Si/PAN composite fibers were prepared by electrospinning. The composite was carbonized by annealing at 800°C for 2 h in Ar atmosphere. Onto the Si/C nanofibers 7-28 ALD cycles of Al_2O_3 were deposited (120°C, TMA and H_2O). The Si-C/Al_2O_3 fibers were tested as anode materials for rechargeable Li ion batteries. The Al_2O_3 coating significantly increased the capacity retention and the coulomb metric efficiency, because it increased the mechanical integrity of the electrode structure and prevented side reactions between the electrode and the electrolyte [81].

4.3. Inorganic core/shell nanofibers produced by electrospinning and ALD

In the last group of composite nanofibers, there is no organic material in the core of the fibers. WO_3/TiO_2 core/shell nanofibers with enhanced visible light photocatalytic activity are good examples for these materials. Polymer/inorganic PVP/ammonium metatunsgstate composite nanofibers were electrospun. They were annealed at 500 °C for 1 h in air to get 250 nm thick WO_3 nanofibers, composed of 20-60 nm interconnected nanoparticles. The authors studied in detail the effect of heating program during annealing and concluded that the polymer/inorganic fibers had to be annealed very slowly (1°C/min) and at the lowest possible temperature, in order to prevent the disintegration of the as-formed oxide fibers into particles [82].On the WO_3 nanofibers 1.5-20 nm TiO_2 thin films were deposited by ALD (250°C, $TiCl_4$ and H_2O) (see figure 6). Under visible light, the WO_3/1.5 nm TiO_2

nanofibers had the highest photocatalytic activity, even higher than Degussa TiO_2, while the thicker TiO_2 layers filled the voids between the NPs of the nanowires and reduced the specific surface area, weakened the photocatalytic activity [83].

The photocatalytic activity of TiO_2 nanofibers was also increased by doping with Nb and depositing Pt nanoparticles onto them. A solution of polyvinyl acetate (PVAc), $Ti(O_iPr)_4$ and $Nb(OEt)_5$ was electrospun, then annealed at 500°C in air for 24 h. As a result, 152-220 nm Nb-doped TiO_2 nanofibers were obtained. Onto them 4-14 nm Pt nanoparticles were deposited by ALD (270°C, $(MeCp)Pt(Me)_3$ and O_2). The hybrid fibers were studied as possible fuel cell anodes. The Nb doping increased the conductivity of TiO_2, and thus the ORR became 20 times higher. A larger Pt load and post-treatment in 5% H_2 at 500°C increased the ORR even further [84].

In another study, it was investigated what happened if the core and shell materials were exchanged in photocatalytic core/shell nanofibers. PVP/$Ti(O_iPr)_4$ and PVP/ZnAc nanofibers were electrospun, then annealed at 500°C in air for 3 h. Then they were covered with ZnO (200°C DEZ and H_2O) and TiO_2 (200°C, $Ti(NMe_2)_4$ and H_2O) thin films by ALD to get 200 nm thick TiO_2/ZnO and 270 thick ZnO/TiO_2 core/shell nanofibers, respectively. These two combinations exposed electrons and holes selectively to the environment, which migrated to TiO_2 and ZnO, respectively. During photocatalysis, the TiO_2/ZnO had considerable higher activity owing to the efficient hole capture by oxygen vacancies, and to the lower mobility of holes [85].

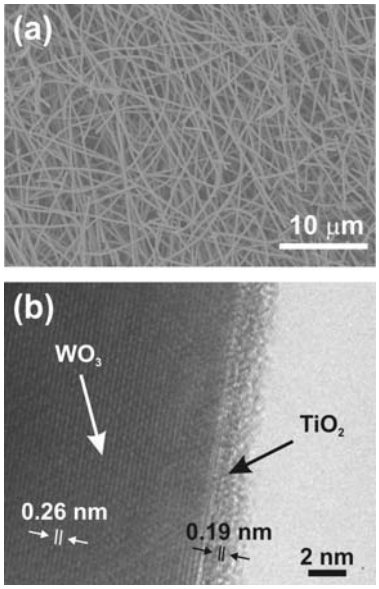

Figure 6. (a) SEM image of electrospun WO_3 nanofibers; (b) HRTEM image of the WO_3/1.5 nm TiO_2 core/shell nanofiberscomposite [83]. (Copyright Wiley-VCH Verlag GmbH & Co. KGaA. Reproduced with permission.)

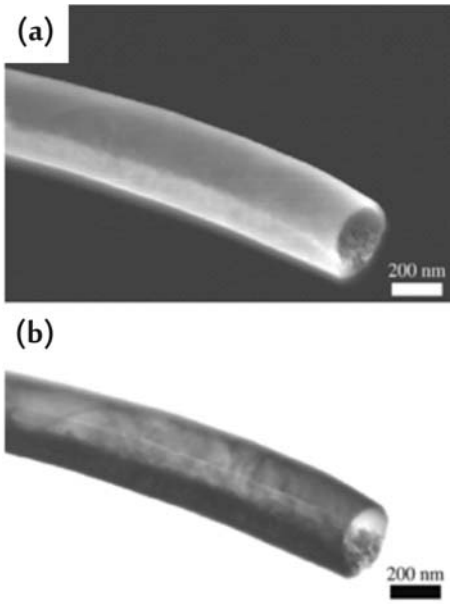

Figure 7. FESEM (a) and STEM (b) images of Fe_2O_3 particle filled TiO nanotube [61]. (DOI: 10.1088/0957-4484/20/3/035602. © IOP Publishing. Reproduced with permission. All rights reserved.)

Reusable magnetic and photocatalytic $CoFe_2O_4$ and Fe_2O_3nanoparticle loaded hollow TiO_2 nanofibers are presented as last examples (figure 7). PVP/$Fe(NO_3)_3$/$Co(NO_3)_2$ and PVP/$Fe(AcO)_2$ polymer/inorganic composite fibers were obtained by electrospinning, onto which TiO_2nanofilms were grown by ALD (250°C, $TiCl_4$ and H_2O). The composites were annealed in air at 500 °C for 4 h to remove the polymer. If the concentrations of the Fe and Co precursors were low enough in the electrospinning solutions, then after annealing the $CoFe_2O_4$ and Fe_2O_3filled only partially the voids of the TiO_2 shells, and nanoparticle loaded nanotubes were prepared. The $CoFe_2O_4$/TiO_2 and

Fe_2O_3/TiO_2composites were good photocatalysts, and after the photocatalytic reaction they could be collected simply by a magnet instead of centrifuging or filtration [61].

5. Conclusion

Electrospinning is an easy and cost-effective way to prepare various nanofibers. ALD has been proven to be a valuable tool not just in semiconductor industry but also in many fields of nanotechnology. Their combination is a powerful way to prepare nanotubes and core/shell nanofibers with tuned properties. The first study on using both electrospinning and ALD to prepare 1D nanostructures was published less than ten years ago, and since then the number of materials prepared by the synergy of these two techniques has increased rapidly.

For electrospinning, such polymers (PVA, PVP, PAN, PEO, nylon, PSU, PVAc) were used, which had some heteroatoms that could serve as nucleation centers for ALD. Onto them usually the most widespread ALD oxide materials (Al_2O_3, ZnO, TiO_2) were deposited, but other oxides (SnO_2, HfO_2) and even noble metals (Pt) were also grown, either by thermal ALD or by PE-ALD.

To obtain nanotubes, the polymer core had to be removed, which was done mostly by annealing, but occasionally also by dissolution or by O_2plasma treatment. In several cases, simple nanotubes (e.g. Al_2O_3, ZnO, TiO_2, SnO_2, HfO_2) were prepared, but also more sophisticated structures (nanotube Al_2O_3yarns, multilayer $Al_2O_3/ZnO/Al_2O_3$, SnO_2/TiO_2 and Ag nanoparticle embedded Al_2O_3/TiO_2 nanotubes) were synthesized.

In the case of many core/shell nanofibers, the as-spun polymer fiber itself served as the core. In many examples, flexible core/shell fiber mats were obtained, which had beneficial mechanical properties. It was shown that depending on their properties, the ALD precursors can diffuse either into the fiber and start nucleation there, or they start to form films only on the surface. By using various precursors and ALD reaction parameters, on the polymer cores Al_2O_3, ZnO and TiO_2 films, and ZnO nanoparticles were grown by ALD, but also hybrid organic/inorganic Al-O-glycidol layers by MLD.In few cases, the polymers contained Fe or Si salts or nanoparticles, and when after the ALD reaction the polymer core was carbonized, and Fe-C/TiO_2 and Si-C/TiO_2 core/shell composites were produced.

When the polymer core was oxidized before the ALD run, inorganic core/shell nanofibers were prepared. When the core inorganic fiber consists of nanoparticles, the ALD layer should be thin in order not to reduce the specific surface by filling the voids between the particles, as was shown by the example of WO_3/TiO_2 composite. When the inorganic salts had lower concentration in the polymer solution, even magnetic nanoparticle loaded hollow Fe_2O_3/TiO_2 or $CoFe_2O_4/TiO_2$ nanofibers could be obtained. With ALD and electrospinning it could be studied what happens if the core and shell materials are exchanged (ZnO/TiO_2, TiO_2/ZnO). Not just films but also nanoparticles could be deposited on the inorganic nanofibers by ALD, as in the case of Nb-doped TiO_2/Pt composites.

The various nanotubes and core/shell nanofibers had versatile applications ranging from photocatalysis and solar cells to batteries, gas sensors and fuel cells. It is clear that the combination of electrospinning and ALD can provide both simple and sophisticated 1D nanostructures as well. The present examples are only to show up the potential in the synergy of these two methods, but there is large room and also need for novel 1D nanomaterials with programmed properties, which predicts a huge development of the field.

6. Acknowledgements

I. M. S. thanks for a János Bolyai Research Fellowship of the Hungarian Academy of Sciences and an OTKA-PD-109129 grant.This paper was presented at INERA Workshop “Transition metal Oxide Films-functionalk layers in “ Smart windows” and Water Splitting Devices”, September 4-6th, 2014, Varna, Bulgaria. The Workshop is part of the Program of INERA REGPOT Project of Institute of Solid State Physics, Bulgarian Academy of Sciences.

References

[1] Yuan J Y and Muller A H E 2010 *Polymer* **51** 4015

[2] Ye J F and Qi L M 2008 *J Mater Sci Tech* **24** 529
[3] Wernersson L E, Thelander C, Lind E and Samuelson L 2010 *Proc IEEE* **98** 2047
[4] Tenne R and Seifert G 2009 *Annu Rev Mater Res* 39 387
[5] Xia Y N, Yang P D, Sun Y G, Wu Y Y, Mayers B, Gates B, Yin Y D, Kim F and Yan Y Q 2003 *Adv Mater* **15** 353
[6] Yang P, Yan R and Fardy M 2010 *Nano Lett* **10** 1529
[7] Tenne R and Rao C N R 2004 *Philos T Roy Soc* A **362** 2099
[8] Jamnik J, Dominko R, Erjavec B, Remskar M, Pintar A and Gaberscek M 2009 *Adv Mater* **21** 2715
[9] Mieszawska A J, Jalilian R, Sumanasekera G U and Zamborini F P 2007 *Small* **3** 722
[10] Ruda H, Polanyi J, Yang J, Wu Z, Philipose U, Xu T, Yang S, Kavanagh K, Liu J, Yang L, Wang Y, Robbie K, Yang J, Kaminska K, Cooke D, Hegmann F, Budz A and Haugen H 2006 *Nanoscale Res Lett* **1** 99
[11] Hernandez-Uresti D B, Sánchez-Martínez D, Martínez-de la Cruz A, Sepúlveda-Guzmán S and Torres-Martínez L M 2014 *Ceram Int* **40** 4767
[12] Zanetti S M, Rocha K O, Rodrigues J A J and Longo E 2014 *Sens Actuat* B **190** 40
[13] Anandan S and Wu J J 2014 *Ultrason Sonochem* **21** 1284
[14] Ramos-Delgado N A, Hinojosa-Reyes L, Guzman-Mar I L, Gracia-Pinilla M A and Hernández-Ramírez A 2013 *Catal Today* **209** 35
[15] Han X, Han X, Li L and Wang C 2012 *New J Chem* **36** 2205
[16] Bai S, Zhang K, Luo R, Li D, Chen A and Liu C C 2012 *J Mater Chem* **22** 12643
[17] Arutanti O, Ogi T, Nandiyanto A B D, Iskandar F and Okuyama K 2014 *AIChE Journal* **60** 41
[18] Luo X, Liu F, Li X, Gao H and Liu G 2013 *Mater Sci Semicon Proc* **16** 1613
[19] Amano F, Ishinaga E and Yamakata A 2013 *J Phys Chem C* **117** 22584
[20] Ritala M and Leskelä M 2002 *Chapter 2 - Atomic layer deposition* in Handbook of Thin Films (Academic Press) 103
[21] Available from: www.aldpulse.com.
[22] Johnson R W, Hultqvist A and Bent S F 2014 *Mater Today* **17** 236
[23] Parsons G N, George S M and Knez M 2011 *MRS Bull* **36** 865
[24] Niinisto L, Paivasaari J, Niinisto J, Putkonen M and Nieminen M 2004 *Phys Status Solidi* A **201** 1443
[25] Cheol Seong Hwang C Y Y 2014 *Atomic Layer Deposition for Semiconductors*: Springer New York Heidelberg Dordrecht London)
[26] Pinna N and Knez M 2011 *Atomic Layer Deposition of Nanostructured Materials* (Weinheim, Germany: Wiley-VCH Verlag & Co. KGaA)
[27] Robertson J 2004 *Eur Phys J-Appl Phys* **28** 265
[28] Leskelä M and Ritala M *J Solid State Chem* **171** 170
[29] George S M 2009 *ChemRev* **110** 111
[30] Puurunen R L 2005 *J Appl Phys* **97** 121301
[31] Zaera F 2013 *Coordin Chem Rev* **257** 3177
[32] Putkonen M, Sajavaara T, Niinisto L and Keinonen J 2005 *Anal Bioanal Chem* **382** 1791
[33] Devi A 2013 *Coordin Chem Rev* **257** 3332
[34] Emslie D J H, Chadha P and Price J S 2013 *Coordin Chem Rev* **257** 3282
[35] Suntola T 1996 *Appl Surf Sci* **100** 391
[36] Niinisto L, Ritala M and Leskela M 1996 *Mat Sci Eng B* **41** 23
[37] Elers K E, Blomberg T, Peussa M, Aitchison B, Haukka S and Marcus S 2006 *ChemVapor Dep* **12** 13
[38] Ritala M 1997 *Appl Surf Sci* **112** 223
[39] Mikko R and Markku L 1999 *Nanotechnology* **10** 19
[40] Miikkulainen V, Leskela M, Ritala M and Puurunen R L 2013 *J Appl Phys* **113** 021301

[41] Lee S W, Choi B J, Eom T, Han J H, Kim S K, Song S J, Lee W and Hwang C S 2013 *Coordin Chem Rev* **257** 3154
[42] Sundberg P and Karppinen M 2014 *Beilstein J Nanotechn* **5** 1104
[43] Hatanpää T, Ritala M and Leskelä M 2013 *Coordin Chem Rev* **257** 3297
[44] Knisley T J, Kalutarage L C and Winter C H 2013 *Coordin Chem Rev* **257** 3222
[45] Ramos K B, Saly M J and Chabal Y J 2013 *Coordin Chem Rev* **257** 3271
[46] Tynell T and Karppinen M 2014 *Semicond Sci Tech* **29** 043001
[47] Putkonen M and Niinistö L 2005 *Organometallic Precursors for Atomic Layer Deposition* in Precursor Chemistry of Advanced Materials (Springer Berlin Heidelberg) 125 p
[48] Parsons G N, Atanasov S E, Dandley E C, Devine C K, Gong B, Jur J S, Lee K, Oldham C J, Peng Q, Spagnola J C and Williams P S 2013 *Coordin Chem Rev* **257** 3323
[49] Ponraj J S, Attolini G and Bosi M 2013 *Crit Rev Solid State* **38** 203
[50] Kim H 2003 *J Vac Sci Technol B* **21** 2231
[51] Knoops H C M, Langereis E, van de Sanden M C M and Kessels W M M 2010 *J Electrochem Soc* **157** G241
[52] Potts S E and Kessels W M M 2013 *Coordin Chem Rev* **257** 3254
[53] Mackus A J M, Bol A A and Kessels W M M 2014 *Nanoscale* **6** 10941
[54] Leskelä M and Ritala M 2002 *Thin Solid Films* **409** 138
[55] Knez M, Nielsch K and Niinistö L 2007 *AdvMater* **19** 3425
[56] Detavernier C, Dendooven J, Sree S P, Ludwig K F and Martens J A 2011 *Chem Soc Rev* **40** 5242
[57] Kim H, Lee H B R and Maeng W J 2009 *Thin Solid Films* **517** 2563
[58] Liu M N, Li X L, Karuturi S K, Tok A I Y and Fan H J 2012 *Nanoscale* **4** 1522
[59] Bakke J R, Pickrahn K L, Brennan T P and Bent S F 2011 *Nanoscale* **3** 3482
[60] Marichy C and Pinna N 2013 *Coordin Chem Rev* **257** 3232
[61] Santala E, Kemell M, Leskela M and Ritala M 2009 *Nanotechnology* **20** 035602
[62] Peng Q, Sun X Y, Spagnola J C, Hyde G K, Spontak R J and Parsons G N 2007 *Nano Lett* **7** 719
[63] Heikkila P, Hirvikorpi T, Hilden H, Sievanen J, Hyvarinen L, Harlin A and Vaha-Nissi M 2012 *J Mater Sci* **47** 3607
[64] Peng Q, Sun X-Y, Spagnola J C, Saquing C, Khan S A, Spontak R J and Parsons G N 2009 *ACS Nano* **3** 546
[65] Kim G-M, Lee S-M, Knez M and Simon P 2014 *Thin Solid Films* **562** 291
[66] Cho S, Kim D H, Lee B S, Jung J, Yu W R, Hong S H and Lee S 2012 *Sensor Actuat B* **162** 300
[67] Kim W S, Lee B S, Kim D H, Kim H C, Yu W R and Hong S H 2010 *Nanotechnology* **21** 245605
[68] Lee B S, Kim W S, Kim D H, Kim H C, Hong S H and Yu W R 2011 *Smart Mater Struct* **20** 105019
[69] Kim G M, Lee S M, Michler G H, Roggendorf H, Gosele U and Knez M 2008 *Chem Mater* **20** 3085
[70] Jung M-H, Yun Y J, Chu M-J and Kang M G 2013 *Chem Eur J* **19** 8543
[71] Jeun J H, Park K Y, Kim D H, Kim W S, Kim H C, Lee B S, Kim H, Yu W R, Kang K and Hong S H 2013 *Nanoscale* **5** 8480
[72] Donmez I, Kayaci F, Ozgit-Akgun C, Uyar T and Biyikli N 2013 *J Alloy Comp* **559** 146
[73] Oldham C J, Gong B, Spagnola J C, Jur J S, Senecal K J, Godfrey T A and Parsons G N 2010 *ECS Transactions* **33** 279
[74] Oldham C J, Gong B, Spagnola J C, Jur J S, Senecal K J, Godfrey T A and Parsons G N 2011 *J Electrochem Soc* **158** D549
[75] Kayaci F, Ozgit-Akgun C, Donmez I, Biyikli N and Uyar T 2012 *ACS Appl Mater Interface* **4** 6185
[76] Kayaci F, Ozgit-Akgun C, Biyikli N and Uyar T 2013 *RSC Adv* **3** 6817

[77] Kayaci F, Vempati S, Donmez I, Biyikli N and Uyar T 2014 *Nanoscale* **6** 10224
[78] Kayaci F, Vempati S, Ozgit-Akgun C, Biyikli N and Uyar T 2014 *Appl Catal B* **156** 173
[79] McClure C D, Oldham C J, Walls H J and Parsons G N 2013 *J Vac Sci Technol A* **31** 061506
[80] McClure J P, Devine C K, Jiang R Z, Chu D, Cuomo J J, Parsons G N and Fedkiw P S 2013 *J Electrochem Soc* **160** F769
[81] Li Y, Sun Y J, Xu G J, Lu Y, Zhang S, Xue L G, Jur J S and Zhang X W 2014 *J Mater Chem A* **2** 11417
[82] Szilágyi I, Santala E, Heikkilä M, Kemell M, Nikitin T, Khriachtchev L, Räsänen M, Ritala M and Leskelä M 2011 *J Therm Anal Calorim* **105** 73
[83] Szilágyi I M, Santala E, Heikkilä M, Pore V, Kemell M, Nikitin T, Teucher G, Firkala T, Khriachtchev L, Räsänen M, Ritala M and Leskelä M 2013 *Chem Vapor Dep* **19** 149
[84] Du Q, Wu J B and Yang H 2014 *ACS Catal* **4** 144
[85] Kayaci F, Vempati S, Ozgit-Akgun C, Donmez I, Biyikli N and Uyar T 2014 *Nanoscale* **6** 5735